MISSOURI S&T

CENTER FOR TRANSPORTATION INFRASTRUCTURE AND SAFETY

Behavior of Hollow-Core FRP-Concrete-Steel Columns Subjected To Cyclic Axial Compression

by

Mohamed Elgawady
and
Omar Abdelkarim

August 2014

NUTC R357

A National University Transportation Center at Missouri University of Science and Technology

Disclaimer

The contents of this report reflect the views of the author(s), who are responsible for the facts and the accuracy of information presented herein. This document is disseminated under the sponsorship of the Department of Transportation, University Transportation Centers Program and the Center for Transportation Infrastructure and Safety NUTC program at the Missouri University of Science and Technology, in the interest of information exchange. The U.S. Government and Center for Transportation Infrastructure and Safety assumes no liability for the contents or use thereof.

Technical Report Documentation Page

1. Report No.	2. Government Accession No.	3. Recipient's Catalog No.
NUTC R357		

4. Title and Subtitle	5. Report Date
Behavior of Hollow-Core FRP-Concrete-Steel Columns Subjected To Cyclic Axial Compression	August 2014
	6. Performing Organization Code

7. Author/s	8. Performing Organization Report No.
Mohamed Elgawady and Omar Abdelkarim	Project #00043006

9. Performing Organization Name and Address	10. Work Unit No. (TRAIS)
Center for Transportation Infrastructure and Safety/NUTC program Missouri University of Science and Technology 220 Engineering Research Lab Rolla, MO 65409	11. Contract or Grant No. DTRT06-G-0014

12. Sponsoring Organization Name and Address	13. Type of Report and Period Covered
U.S. Department of Transportation Research and Innovative Technology Administration 1200 New Jersey Avenue, SE Washington, DC 20590	Final
	14. Sponsoring Agency Code

15. Supplementary Notes

16. Abstract

This report presents the results of an experimental study that was conducted to investigate the effects of key parameters on the compressive behavior of fiber reinforced polymer (FRP)-concrete-steel double-skin tubular columns (FSDT). Hybrid FSDT columns have been introduced as a new form of hybrid columns. They consist of an outer tube made of FRP and inner tube made of steel, with sandwiched concrete between them. This report investigated the effect of fiber angle and the ratio of steel tube diameter to its thickness (Di/ts) on the compressive behavior of FSDT columns. Ten FSDT cylinders with different (Di/ts) in addition to three concrete filled-fiber tuber (CFFT) cylinders were manufactured and tested under axial cyclic compression. The results of the experimental study indicate that the overall behavior of FSDT and CFFT is similar and the main difference is in the capacity load. The cylinders with high D/t ratio achieve lower capacity than the normal capacity due to the local buckling of the steel tubes. Using the saturated fiber tube increases the axial ductility but does not give high confinement. These results are presented together with a discussion on the influence of the studied parameters on the compressive behavior of FSDTs.

17. Key Words	18. Distribution Statement
words	No restrictions. This document is available to the public through the National Technical Information Service, Springfield, Virginia 22161.

19. Security Classification (of this report)	20. Security Classification (of this page)	21. No. Of Pages	22. Price
unclassified	unclassified	22	

Form DOT F 1700.7 (8-72)

Behavior of Hollow-Core FRP-Concrete-Steel Columns Subjected To Cyclic Axial Compression

ABSTRACT

This report presents the results of an experimental study that was conducted to investigate the effects of key parameters on the compressive behavior of fiber reinforced polymer (FRP)-concrete-steel double-skin tubular columns (FSDT). Hybrid FSDT columns have been introduced as a new form of hybrid columns. They consist of an outer tube made of FRP and inner tube made of steel, with sandwiched concrete between them. This report investigated the effect of fiber angle and the ratio of steel tube diameter to its thickness (D_i/t_s) on the compressive behavior of FSDT columns. Ten FSDT cylinders with different (D_i/t_s) in addition to three concrete filled-fiber tuber (CFFT) cylinders were manufactured and tested under axial cyclic compression. The results of the experimental study indicate that the overall behavior of FSDT and CFFT is similar and the main difference is in the capacity load. The cylinders with high D/t ratio achieve lower capacity than the normal capacity due to the local buckling of the steel tubes. Using the saturated fiber tube increases the axial ductility but does not give high confinement. These results are presented together with a discussion on the influence of the studied parameters on the compressive behavior of FSDTs.

Table of Contents

1 INTRODUCTION

In the last few decades, concrete filled fiber tubes (CFFT) have been widely used in USA, Japan, China, and Europe. Fiber reinforced polymer (FRP) tubes have gained acceptance as an alternative to steel tubes in concrete filled steel tubes (CFST). CFFTs have many advantages such as light weight-to-strength ratio, high confinement and corrosion resistance compared to steel tubes. Seismic behavior of CFFT columns has been studied (e.g. Shin and Andrawes 2010, Zhu et al. 2006). Dawood et al. (2012) and ElGawady and Sha'lan (2011), ElGawady et al. (2010) have studied the CFFT columns under seismic loading as well.

Montague (1978) developed another version of concrete filled tubular columns, namely double-skin tubular column (DSTC). A DSTC consists of two generally concentric steel tubes with concrete poured between them to form the core of the sandwich. Many researchers investigated the behavior of DSTCs (e.g. Shakir-Khalil and Illouli 1987, Yagishita 2000; Han et al. 2006). Recently, Teng et al. (2004) used FRP as the outer tube of double skin tubular elements. This system combines and optimizes the benefits of the three materials FRP, concrete, and steel. In recent years, many researchers have been studied the behavior of FRP-steel double skin tubes (FSDT) under different static loadings conditions. The behavior of FSDTs columns and beams has been studied by Teng and his research group (Teng et al. 2005; Yu et al. 2006; Wong et. al 2008; Yu et al. 2010). Han et al. (2010) tested FSDTs in a beam-column arrangement under cyclic flexural loading. More recently, Zhang et al. (2012) investigated the behavior of small scale FSDTs under combined axial compression and lateral cyclic loading. The results of the conducted experimental tests under axial compression, flexure and combined axial compression and flexure showed high concrete confinement and ductility.

In FSDT system, the concrete wall thickness between the outer FRP tube and the inner steel tube is usually small, hence self-consolidating concrete (SCC) will represent a good option to avoid honey comb is preferable to be used to lessen the problem of consolidating and vibrating the concrete. SCC has a high flowability and a moderate viscosity that give the ability of self-consolidation. A balance should be achieved between dosages of superplasticizers or high range water reducers (HRWR) for increasing the flowability and dosages of viscosity modifying agents (VMA) to enhance the stability, reducing segregation (Khayat 1999).

2 EXPERIMENTAL PROGRAM

2.1 Test Specimens

In total, thirteen specimens were investigated during the course of this research (table 1 and figure 1) prepared and tested, including ten hybrid FSDT cylinders and three CFFT cylinders. The thirteen specimens were sorted in four groups. FSDTs were prepared with inner steel tubes of three different diameters of 2, 3 and 4 in. Each specimen had outer FRP tube with fiber oriented at ± 45° or hybrid of ± 45°/0°. By definition CFFT has no steel tube. The FRP tubes in group 1 were prepared using carbon fiber (CFRP) and in group 2 were prepared using glass fiber (GFRP), however groups 3 and 4 were prepared using hybrid FRP. All specimens were tested under axial cyclic loading.

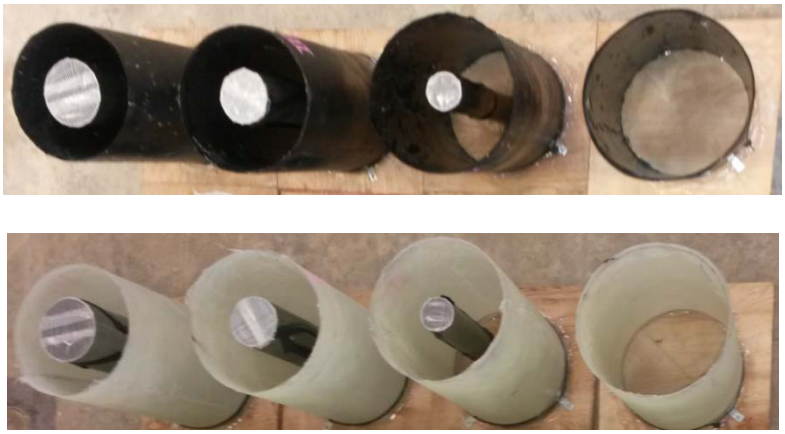

Figure 1: Ready for concrete pouring of FSDTs and CFFTs

The specimens had an outer diameter of 8.25 inch and a height of 16 inch. The FRP tubes were prepared manually by a wet-layup process on sonotube and were used as a mold for concrete pouring. The last wrapped layer of FRP tube was provided with 30% overlap to prevent premature debonding failure. The studied parameters were the ratio of the steel tube diameter to its thickness (D/t) and using different type of fibers. Table 1 shows the specimens details.

2.2 Material Properties

Table 2 shows the mix design of the used SCC. The average cylindrical concrete compressive strength (f_c') at 56 days is 8,000 psi for five standard cylinders 6" x 12". One of these cylinders was tested under cyclic loading as explained later in this report and the others were tested under monotonic loading with a displacement rate of 0.02 in/min.

Table 1: Specimens descriptions

Group No.	Specimen Number	Outer FRP tube	Inner steel tube D_i (t_s) (inch)	Concrete cylindrical strength f_c' (psi)
1	DS-CIII45-64	CFRP- Three layers 45^o	4.00 (0.063)	8,000
	DS-CIII45-39		3.00 (0.077)	
	DS-CIII45-32		2.00 (0.063)	
	CFFT-CIII45		-	
2	DS-GIII45-64	GFRP- Three layers 45^o	4.00 (0.063)	8,000
	DS-GIII45-39		3.00 (0.077)	
	DS-GIII45-32		2.00 (0.063)	
	CFFT-GIII45		-	
3	DS-GII45-GI0-64	Hybrid GFRP- Two layers 45^o + One Layer 0^o	4.00 (0.063)	8,000
	DS-GII45-GI0-39		3.00 (0.077)	
	DS-GII45-GI0-32		2.00 (0.063)	
	CFFT-GII45-GI0		-	
4	DS-GI45-GII0-64	Hybrid GFRP- One layer 45^o + Two Layers 0^o	4.00 (0.063)	8,000

Table 2: SCC mixture proportions

w/cm	Cement (lb/cy)	Fly Ash (lb/cy)	Water (lb/cy)	Fine aggregate (lb/cy)	Coarse aggregate (lb/cy)	HRWRA (lb/cy)	VEA (lb/cy)
0.38	590	295	336	1411	1411	3.6	1.2

Standard coupons were cut longitudinally from the steel tube for tensile tests according to ASTM A1067. The steel coupon tests were conducted under a displacement control of 0.03 in/min. A strain gauge was attached to the mid height of the steel coupons (Figure 2(a)). All steel coupons failed by yielding neck. The average stress-strain curve of steel coupons is shown in figure 3. The results showed that the yield stress, tensile stress and the Young's modulus of the steel tubes are 90,000 psi, 90,000 psi, 29,000 ksi respectively.

Three hollow steel tubes similar to those used in the DS were tested under monotonic axial compression. Two strain gauges in the hoop direction and two vertical strain gauges were mounted on the outer surfaces of steel tubes as shown in figure 2 (b). Steel tubes A and B failed by the local buckling in the elephant's foot mode at ultimate loads 67.80 kips and 66.50 kips, respectively. This is corresponding to stresses of 85.78 ksi and 89.42 ksi, respectively. However the steel tube C failed by global buckling and the local buckling in the elephant's foot mode at load 18.55 kips corresponding to a stress of 45.81 ksi. Failure load of tube C was significantly lower than the other tubes because the global buckling occurred early (Figure 2 (c)).

According to ASTM D3039, longitudinal and radial coupons were cut from the one layer FRP tubes. One horizontal and one vertical strain gauge were attached to the mid height of the longitudinal FRP coupon as shown in figure 4 (a). Two strain gauges were attached to the mid of the radial disk as shown in figure 4 (b). Under tensile tests with a displacement loading rate of 0.05 in/min, all FRP coupons whether longitudinal or radial failed by debonding between the two

45^{o} plies [+45^{o} and -45^{o}] without fiber rupture as shown in figure 4. The ultimate stress was 10,500 psi (Figure 5). The saturated FRP with fiber orientation at 45o has a structure depends on fibers in two perpendicular directions [+45^{o} and -45^{o}] and adhesive material between them. Therefore this type of laminates works globally. As a result, the fibers did not work in the coupon tests as the width of the strip is only 1 inch so there is no fibers continuity. The properties of the FRP here were referenced based on the manufacturer data sheet (Table 4).

(a) (b) (c)

Figure 2: (a) steel coupon during tensile test, (b) Steel tube A during compression test; (c) Failure modes of the steel tubes A, B and C

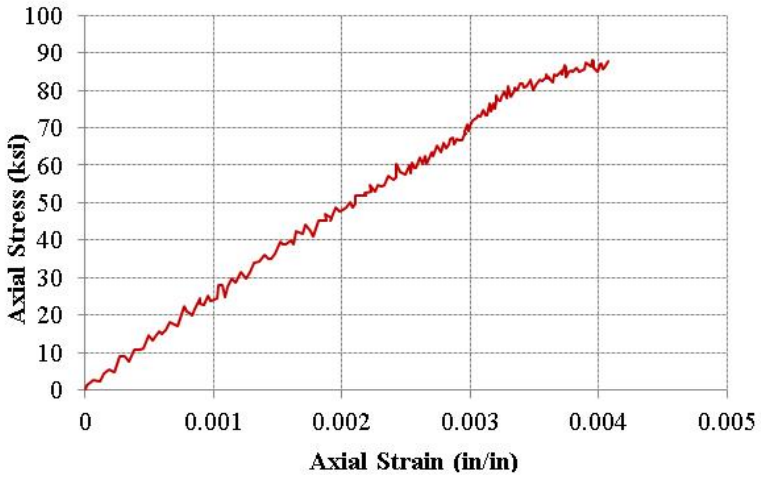

Figure 3: Axial strain-stress curve for steel coupon tensile test

Table 3: Properties of steel tubes

Material	Young's modulus, E (ksi)	Yield stress (psi)	Ultimate stress (psi)	Ultimate strain
Steel	29,000	90,000	90,000	0.40 %

Table 4: Properties of saturated FRP according to manufacturer's data

Material	Nominal thickness/layer (in)	Young's modulus, E (ksi)	Tensile strength (psi)	Ultimate strain
CFRP-45^{o}	0.034	6,950	95,850	1.40 %
GFRP-45^{o}	0.034	2,700	40,500	1.50 %
GFRP-0^{o}	0.050	3,790	83,400	2.20 %

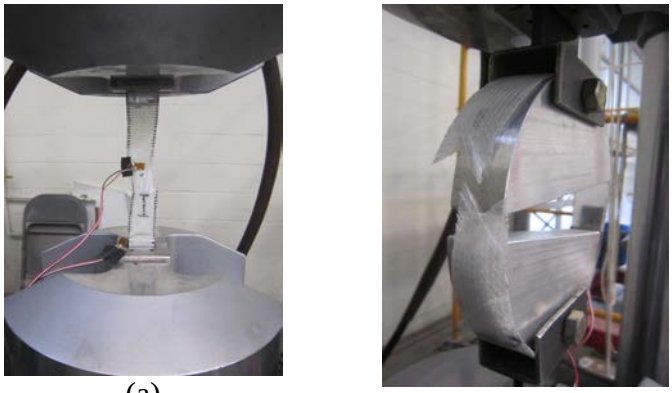

(a) (b)

Figure 4: (a) Longitudinal FRP coupon; (b) Radial FRP coupon

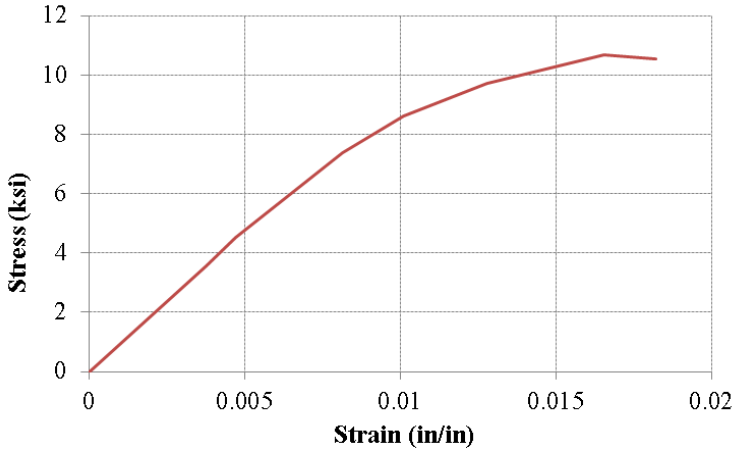

Figure 5: Strain-stress curve for FRP radial coupon

2.3 Experimental Set-up and Instrumentation

Compression tests were carried out using MTS machine with a loading rate of 0.02 inch/min. All test data, including the strains, loads, and displacements, were recorded simultaneously using a data acquisition system. Two horizontal and two vertical strain gauges were installed on the outer surface at the mid-height of the FRP tube. Likewise two horizontal and two vertical strain gauges were installed on the outer surface at the mid-height of the steel tube. In addition, two string potentiometers were attached on the outer surface of the FRP tube to obtain the axial deformation of the middle region of 5.5 in for each specimen. Another radial string potentiometer was installed around the outer surface of the cylinder at the mid height in order to measure the average hoop strain.

2.4 Loading Schemes

All specimens were tested under compression loading on cyclic scheme as shown in figure 6. The cyclic compression involved full loading/unloading cycles, where the unloading of each cycle was designed to terminate at a 100 lb (near zero) and the reloading of each cycle was designed to terminate at the unloading displacement of the same cycle. The loading scheme followed nine steps started at axial strain of 0.125 % and was increased gradually until failure of the specimen. Each loading step repeated three cycles.

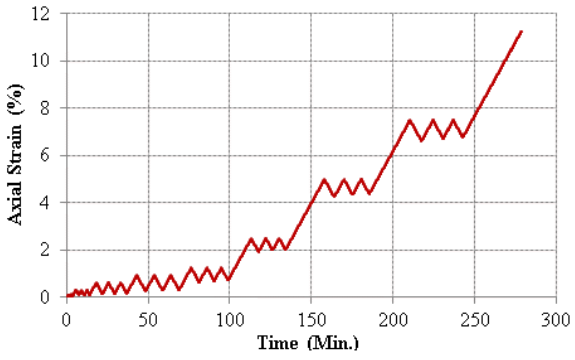

Figure 6: Cyclic loading scheme

3 RESULTS AND DISCUSSIONS OF COMPRESSION TESTS

3.1 General Behavior

The envelope axial strain-load and the hoop strain-load curves of the cyclic curves of groups 1 to 4 are shown in figure 7. All specimens had the same initial stiffness up to reaching the ultimate load. It was clear that this initial part had only one slope up to the ultimate load. The reason for that was the effect of the 45^o FRP. The angle-ply FRP has an ability to give high ductility by the reorientation phenomenon (Au and Buyukozturk 2005). Under axial loading, the angular fiber reoriented from the initial case (+45/-45) toward the hoop direction without rupture. Therefore, the cylinders reached to the ultimate load without fiber rupture.

All specimens failed due to steel tube buckling. The axial strains were obtained from the average readings of the two string potentiometers. The radial strains were calculated using the difference in length of radial string potentiometers versus the initial reading. As shown in figure 7(a) that all specimens in group 1 had similar overall behavior. All of them reached to the maximum MTS machine axial displacement without FRP rupture. The overall hoop strain could not be recorded in specimens DS-CIII45-32 and CFFT-CIII45 as the radial string potentiometer failed early on the test. However it can be noted from figure 7(b) that the specimens behave similarly in the hoop direction. While the local buckling occurred in the inner steel tubes in all specimens even in the tube with the smaller diameter as shown in figure 8 (c). The effect of steel tube local buckling will be studied later in this report. In general, the specimens in this group achieved high axial strain around 0.12 and high hoop strain around 0.05.

The overall behaviors of the specimens in group 2 were very similar to the ones in group 1. However, all specimens in this group were ruptured before reaching the maximum applied axial strain except DS-GIII45-64 as the maximum applied strain was lower than the others. It can be concluded that the GFRP was reorienting faster than the CFRP hence the fibers were much

closer to the hoop direction after the reorientation. That explained also why the specimens in group 2 achieved higher capacities than the ones in group 1. Figure 8 shows the failure of the specimens in group 1 and 2.

The specimens of groups 3 & 4 of hybrid FRP had the same behavior to fail. The capacities of all cylinders of these groups were higher than the nominal capacity. The initial stiffness of the DS cylinders was almost the same however the CFFT had higher initial stiffness. When the outer unidirectional FRP layers ruptured, the axial strength dropped to 35-40% of the capacity at axial strain approximately of 0.02. After that, the angle-ply FRP layers kept the residual strength to approximately strain of 0.04 because of the fiber reorientation. Then, the axial strength reduced slowly with the increase of the axial strain up to approximately of 0.11.

3.2 Axial-hoop strains relation

The relation between the axial and hoop strain is considered as the key parameter which controls the effectiveness of the confinement of FRP. As all specimens were similar in the relation of the axial and hoop strains, the specimen DS-CIII45-64 was considered for representing this relation. Figure 9 shows the axial strain-load curve and the hoop strain-load curve of such specimen. It was noted that the axial and hoop strains were increasing simultaneously. During the first cycles, before ultimate load, the hoop and axial strains were increasing with high rate. It means the expansion of the concrete under axial loading was outward only. At ultimate load, the failure occurred due to the steel tube local buckling. After the local buckling of the steel tube and up to axial strain of 0.02, the hoop strain was increasing with low rate. It means the concrete expansion was in the outward and inward directions. After the axial strain 0.02, the effect of local buckling almost stopped as the local buckling occurred at

many places in the steel. Therefore, the load slightly increased and the hoop strain was increasing with a moderate rate up to the maximum applied strain.

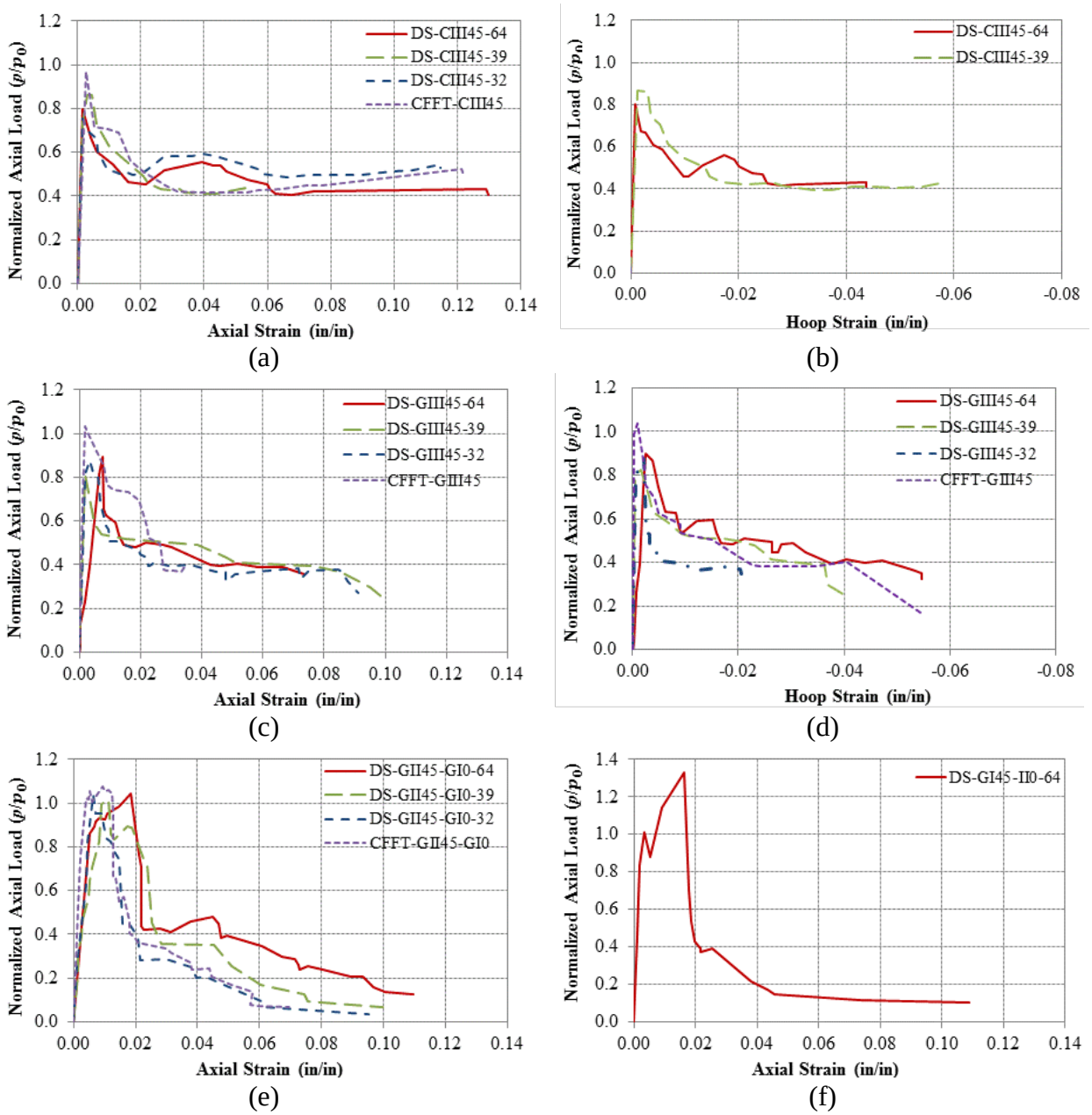

Figure 7: Axial strain-load and hoop strain-load relations for groups 1 to 4

(a) (b) (c) (d)

Figure 8: (a) Group 1 failed specimen, (b) Group 2 failed specimen (c) Steel tube local buckling, (d) Group 3 failed specimen

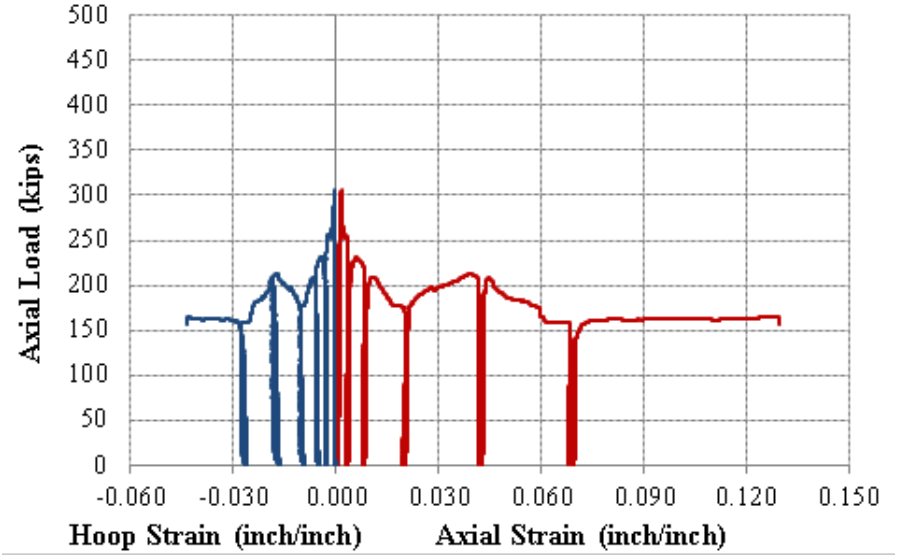

Figure 9: Axial load-strain curve of DS-CIII45-64

3.3 Local buckling of the steel tubes

Study the effect of using D/t ratio is very significant parameter for such columns. Researchers studied FSDT columns with D/t ratio (Ozbakkaloglu 2013, Yu 2010 and 2004, and Wong 2007) as listed in table 5. In general an increase in capacity for such cylinders was achieved or at least no reduction in capacity. Hence, this report presents higher values of this ratio starts with 32 up to 64. The capacity of the tested cylinders ranged by factors of 0.76 to 1.30 from the nominal capacity Po which was calculated by the following equation:

$$P_o = A_s f_y + A_c f_c'$$

The reduction can be explained because of the steel local buckling. However, the vertical strain in the steel tubes of the tested cylinders before local buckling was around 600-800 microstrain which was very low value. That exhibited the low contribution of the steel tube in axial capacity and hence a reduction in capacity occurred.

Normalized D_i/t_s can be defined as the ratio between the D_i/t_s to the D_i/t_s of AISC for the steel hollow section under compression as per the following equation:

$$Normalized\ (^{D_i}/_{t_s}) = {}^{D_i}/_{t_s}\ /(0.07\ \frac{E}{F_y})$$

The local buckling occurs when the D/t ratio is higher than the AISC manual value. The D/t ratio for the tested cylinder relative to the AISC manual value was between 1.37 and 2.74. However this ratio in the cylinders of literature relative to the AISC manual was lower than 1.00 as shown in figure 10. That explained occurring the local buckling in the tested cylinders even in the cylinders with steel tube D/t ratio equals to 32. According to these results presented in this report, the contribution of the steel tube in the nominal capacity calculation should be adjusted therefore this research in continuing for this scope.

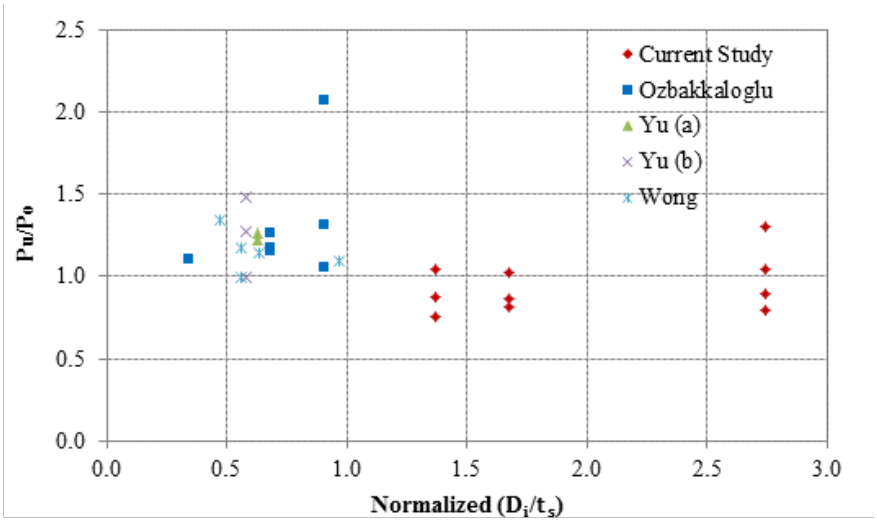

Figure 10: Actual steel diameter-thickness ratios relative to the AISC manual value versus increase in capacity

Table 5: Steel tube D/t ratio of FSDT columns of literature and of our work

	D_o (in)	D_i (in)	t_s (in)	D_i/t_s	$(D_i/t_s)_{AISC}$	Normalized (D_i/t_s)	P_u/P_o
Current Study	8.25	4.00	0.063	64.00	23.33	2.74	0.80
		4.00	0.063	64.00	23.33	2.74	0.89
		4.00	0.063	64.00	23.33	2.74	1.04
		4.00	0.063	64.00	23.33	2.74	1.30
		3.00	0.077	39.00	23.33	1.67	0.86
		3.00	0.077	39.00	23.33	1.67	0.82
		3.00	0.077	39.00	23.33	1.67	1.02
		2.00	0.063	32.00	23.33	1.37	0.76
		2.00	0.063	32.00	23.33	1.37	0.87
		2.00	0.063	32.00	23.33	1.37	1.04
Ozbakkaloglu (2013)	5.91	4.00	0.126	31.75	35.00	0.91	1.31
		4.00	0.126	31.75	35.00	0.91	2.07
		4.00	0.126	31.75	35.00	0.91	1.05
		3.00	0.126	23.78	35.00	0.68	1.16
		3.00	0.126	23.78	35.00	0.68	1.17
		1.50	0.126	11.91	35.00	0.34	1.10
		1.50	0.063	23.81	35.00	0.68	1.27
		1.50	0.063	23.81	35.00	0.68	1.16
Yu (a) (2012)	8.08	5.52	0.209	26.47	42.06	0.63	1.26
						0.63	1.23
Yu (b) (2004)	6.00	3.00	0.126	23.78	41.14	0.58	0.99
						0.58	1.27
						0.58	1.48
Wong (2007)	6.00	1.65	0.091	18.26	38.66	0.47	1.35
		2.99	0.130	23.03	41.14	0.56	0.99
		2.99	0.138	21.71	34.24	0.63	1.14
		3.46	0.083	41.90	43.29	0.97	1.10
		4.53	0.205	22.12	39.52	0.56	1.17

4 CONCLUSIONS

This report has presented the effect of using steel tubes with different D/t ratio and the effect of using angle-plied and hybrid FRP tubes as well in FSDTs. The overall behavior of FSDT is the same and the main difference is in the capacity load. Using angle-plied FRP tube exhibits high level of axial ductility prior to the FRP rupture. Using the hybrid FRP tube (angle-plied and unidirectional) exhibits high axial strength and ductility and the failure is in two stages. The reorientation of the angle-plied FRP tube is very effective on the axial ductility and the capacity. FSDT columns with highly D/t ratio steel tubes have lower capacity than the nominal capacity. The local buckling of the steel tube affects the overall hoop strain of the FRP tube.

5 ACKNOWLEDGEMENT

This research was conducted by Missouri University of Science and Technology and was supported by National University Transportation Center (NUTC). This support is gratefully appreciated. However, any opinions, findings, conclusions, and recommendations presented in this report are those of the authors and do not necessarily reflect the views of sponsors.

6 REFERENCES

ASTM Standard A1067, 2012, "Test Coupons for Steel Castings," ASTM International, West Conshohocken, PA, 2012, 10.1520/A1067_A1067M-12A.

ASTM Standard D3039, 2008, Standard Test Method for Tensile Properties of Polymer Matrix Composite Materials," ASTM International, West Conshohocken, PA, 2008, 10.1520/D3039_D3039M-08.

Au, C. and Buyukozturk, O. (2005). ”Effect of Fiber Orientation and Ply Mix on Fiber Reinforced Polymer-Confined Concrete.” J. Compos. Constr., 9(5), 397–407.

Dawood, H., ElGawady, M. (2013). “Performance-based seismic design of unbonded precast post-tensioned concrete filled GFRP tube piers” Composites Part B: Engineering, Volume 44, Issue 1, Pages 357-367

Dawood, H., ElGawady, M., and Hewes, J. (2012). “Behavior of Segmental Precast Post-Tensioned Bridge Piers under Lateral Loads”, ASCE Journal of Bridge Engineering, Vol. 17, No. 5, pp. 735-746.

ElGawady, M. and Sha’lan, A. (2011). ”Seismic Behavior of Self-Centering Precast Segmental Bridge Bents.” J. Bridge Eng., 16(3), 328–339.

ElGawady, M., Booker, A., and Dawood, H. (2010). ”Seismic Behavior of Posttensioned Concrete-Filled Fiber Tubes.” J. Compos. Constr., 14(5), 616–628.

Han L.H., Huang H., Tao Z. and Zhao X.L. (2006). “Concrete-filled double skin steel tubular (CFDST) beam-columns subjected to cyclic bending”, Engineering Structures, Vol.28, No.12, 1698–714.

Han, L.H., Tao, Z., Liao, F.Y., and Xu, Y. (2010). “Tests on Cyclic Performance of FRP-Concrete –Steel Double-Skin Tubular Columns.” *Thin-Walled Structures*, 4, 430-439.

Khayat KH, Workability, Testing, and Performance of Self-Consolidating Concrete, ACI Materials Journal 1999, 96 (3), 346-354.

Montague, P., (1978). “Experimental behavior of double-skinned, composite, circular cylindrical-shells under external-pressure”. Journal of Mechanical Engineering Science, 20(1), pp. 21–34.

Ozbakkaloglu, T. and Fanggi, B. (2013). "Axial Compressive Behavior of FRP-Concrete-Steel Double-Skin Tubular Columns Made of Normal- and High-Strength Concrete." J. Compos. Constr., 10.1061/(ASCE)CC.1943-5614.0000401 , 04013027.

Shakir-Khalil, H., and Illouli, S.1987. “Composite columns of concentric steel tubes.” Proc., Conf. on the Design and Construction of Non-Conventional Structures, Vol. 1, London, pp. 73–82.

Shin, M. and Andrawes, B. (2010). “Experimental Investigation of Actively Confined Concrete Using ShapeMemory Alloys”. J. Eng. Struct. 32:3, 656-664.

Teng, J.G., Yu, T., and Wong, Y.L. (2004). “Behavior of Hybrid FRP-Concrete-Steel Double-Skin Tubular Columns.” *Proc. 2nd Int. Conf. on FRP Composites in Civil Engineering*, Adelaide, Australia, 811-818.

Teng, J.G., Yu, T., Wong, Y.L., and Dong, S.L. (2005). “Innovative FRP-Steel-Concrete Hybrid Columns.” Advances in Steel Structures, 1, 545-554.

Wong,Y.L., Yu, T., Teng, J.G., and Dong, S.L. (2008). “Behavior of FRP-confined Concrete in Annular Section Columns.”, *Composites: Part B Engineering*, 39, 451-466.

Yagishita F, Kitoh H, Sugimoto M, Tanihira T, Sonoda K. Double-skin composite tubular columns subjected cyclic horizontal force and constant axial force. Proceedings of the Sixth ASCCS Conference, Los Angeles, USA, March 22–24. 2000, p. 497–503.

Yu, T., Cao, Y., Zhang, B. & Teng, J. G. (2012). Hybrid FRP-concrete-steel double-skin tubular columns: Cyclic axial compression tests. 6th International Conference on FRP Composites in Civil Engineering (pp. 1-8).

Yu, T., Wong, Y.L., Teng, J.G., Dong, S.L., and Lam, E.S.S (2006). “Flexural Behavior of Hybrid FRP-Concrete-Steel Double Skin Tubular Members.” *Journal of Composites for Construction*, 10:5, 443-452.

Yu, T., Wong, Y.L., Teng, J.G., and Dong, S.L., (2004). “Structural behavior of hybrid FRP-concrete-steel double-skin tubular columns.” ANCER Annual Meeting: Networking of Young Earthquake Engineering Researchers and Professionals, Honolulu, Hawaii

Yu T, Wong YL, Teng JG. (2010). “Behavior of hybrid FRP-concrete-steel double-skin tubular columns subjected to eccentric compression.” *Advances in Structural Engineering*; 13(5):961-74.

Zhang, B., Teng, J. G. and Yu, T. (2012). “Behaviour of hybrid double-skin tubular columns subjected to combined axial compression and cyclic lateral loading.” *Sixth International Conference on FRP Composites in Civil Engineering* (pp. 1-7). Rome, Italy.

Zhu, Z., Ahmad, I., and Mirmiran, A. (2006). “Seismic performance ofconcrete-filled FRP tube columns for bridge substructure.” J. Bridge Eng., 11(3), 359–370.